Role of Distribution Factors in Congestion Revenue Rights Applications

Minghai Liu, *Student Member, IEEE,* and George Gross, *Fellow, IEEE*

***Abstract*—In the locational marginal price (*LMP*)-based congestion management scheme, transmission customers face uncertainty in the congestion charges they incur. In order to bring certainty to customers, congestion revenue rights (*CRR*) such as the fixed transmission rights (*FTR*) used in the *PJM* interconnection and flowgate rights (*FGR*) are introduced. These *CRR* are financial tools that provide the holder reimbursement of the congestion charges incurred in the day-ahead market. The implementation of *CRR* requires appropriate modeling of the transmission network in which the distribution factors are extensively used. These factors—the injection shift factors (*ISF*s) and the power transfer distribution factors (*PTDF*s)—are linear approximations of the sensitivities of the active power line flows with respect to various variables. The factors are computed for a specified network topology and parameter values. In practice, the *PTDF*s used for the *CRR* issuance may be different from those used in the day-ahead market due to changes in the forecasted network conditions. The *PTDF* errors may impact the *FTR* issuance quantities, the revenue adequacy of the *FTR* issuer and the hedging ability of the *FGR*. In this paper, we explore analytical characteristics of these distribution factors and investigate their role in *CRR* applications. We study the nature of the *PTDF* errors and examine their impacts in these applications, both analytically and experimentally. Our results indicate that the impacts of the *PTDF* errors in *CRR* applications stay in an acceptable range under a broad spectrum of conditions including contingencies used to establish $n-1$ *security*.**

***Index Terms*—Congestion management, congestion revenue rights, distribution factors, fixed transmission rights, flowgate rights, locational marginal prices.**

I. Introduction

OPEN access to the transmission network has resulted in new challenges in the management of the transmission system. Congestion in the transmission network is a key obstacle to vibrant competitive electricity markets. Various schemes have been proposed to manage transmission congestion [1]–[4]. Relying on experiences in specific jurisdictions, the Federal Energy Regulatory Commission (*FERC*) outlined a scheme based on locational marginal prices (*LMP*s) in its standard market design (*SMD*) proposal [4]. In this proposal, an independent entity is established to carry out the responsibilities for the operations and control of the transmission system as well as the management of various markets. We refer to this entity by the generic name of independent grid operator (*IGO*) to encompass various organizations such as independent system operator (*ISO*), transmission system operator (*TSO*), regional transmission organization (*RTO*) and independent transmission provider (*ITP*). At the very minimum, an integrated day-ahead market is operated by the *IGO* in which the *LMP*s are determined for each network node and the presence of congestion is signaled by the *LMP* differences. Congestion charges evaluated in terms of the *LMP* differences are collected by the *IGO* from the market participants.

Since the *LMP*s are unknown before the day-ahead market clears, there is uncertainty in the amount of congestion charges faced by transmission customers. Such uncertainty may make *risk-averse* [5] customers unwilling to undertake transactions unless financial tools were available to *hedge* [5] against such charges. Congestion revenue rights (*CRR*) are financial tools specifically aimed at meeting such a need. *CRR* are issued by the *IGO* and provide the holder reimbursement of the congestion charges collected by the *IGO* in the day-ahead market. Several types of *CRR* have been proposed and implemented under various market structures [4], [6]–[8].

Successful deployment of *CRR* requires appropriate modeling of the transmission network. The models currently in use have, in common, their reliance on the distribution factors. These distribution factors—the injection shift factors (*ISF*s) and the power transfer distribution factors (*PTDF*s)—are linear approximations of the first order sensitivities of the active power flows with respect to various variables [9]–[11]. They have been applied to congestion modeling and their effectiveness in these applications has been investigated [12]. An insightful characterization of these factors—their insensitivity to the system loadings under certain conditions—is given in [13]. Their values are then determined solely by the network topology and parameter values. However, when the *CRR* are issued or sold, the network conditions of the future periods are unknown. Factors computed based on the forecasted operating conditions are used instead. As a result, the factors used for the *CRR* issuance may be different from those used in the day-ahead market. Such differences give rise to questions regarding the robustness of these factors in *CRR* applications.

This paper provides a systematic study on the role and effectiveness of the distribution factors in *CRR* applications. We start with the derivation of the distribution factors and then analyze their characteristics and investigate their role in *CRR* applications. Our focus is on two specific tools, the so-called fixed transmission rights (*FTR*) [6], [7] and the flowgate rights (*FGR*) [8]. We examine the range of conditions over which the distribution factors can provide a reliable approximation for large-scale power system networks. In particular, we evaluate the errors in *ISF*s and *PTDF*s due to contingencies and investigate

Manuscript received June 27, 2003. This work was supported in part by NSF Project 0000577 and in part by PSERC and CERTS.

The authors are with the Department of Electrical and Computer Engineering, University of Illinois at Urbana-Champaign, Urbana, IL 61801 USA (e-mail: mliu@uiuc.edu).

Digital Object Identifier 10.1109/TPWRS.2004.826708

the impacts of these errors on some important aspects of *CRR* deployment: the determination of *FTR* issuance quantities, the guarantee of the *IGO* revenue adequacy, the reconfiguration of existing *CRR*, and the construction of *FGR* portfolios. We establish analytical bounds for the relative errors of these outcomes and illustrate them with numerical studies on various systems. These studies demonstrate the robustness of the *ISF*s and *PTDF*s in *CRR* applications under a variety of system conditions and parameter values.

This paper consists of five additional sections. Section II reviews the definition and characteristics of the distribution factors. In Section III, the role of the distribution factors in *CRR* applications is discussed. We devote Section IV to analyze the *PTDF* errors due to changes in the network topology/parameters and evaluate their impacts in *CRR* applications. We show representative numerical results in Section V using systems derived from the IEEE 118-bus system and portions of the Eastern Interconnection of the U.S.

II. Basic Distribution Factors

We consider a power system with $N+1$ buses and L lines. We denote by $\mathcal{N} \triangleq \{0, 1, 2, \ldots, N\}$ the set of buses, with the bus 0 being the slack bus, and by $\mathcal{L} \triangleq \{\ell_1, \ell_2, \ldots, \ell_L\}$ the set of transmission lines and transformers that connect the buses in the set $\mathcal{N}$. We associate with each element $\ell \in \mathcal{L}$ the *ordered* pair $\ell = (i, j)$ with the convention that the direction of the flow in line ℓ is *from* node i *to* node j so that $f_\ell \geq 0$, where f_ℓ is the active power flow in line ℓ. We define $\underline{\boldsymbol{f}} \triangleq [f_1, f_2, \ldots, f_L]^T$. The series admittance of line ℓ is $g_\ell - jb_\ell$. We denote the net active (reactive) power injection at node $n \in \mathcal{N}$ by $p_n(q_n)$ and define $\underline{\boldsymbol{p}} \triangleq [p_1, p_2, \ldots, p_N]^T (\underline{\boldsymbol{q}} \triangleq [q_1, q_2, \ldots, q_N]^T)$. We represent the basic transaction with receipt point (*from* node) m, delivery point (*to* node) n in the amount t *MW* by the *ordered* triplet $\omega \triangleq \{m, n, t\}$. Let $\mathcal{W} \triangleq \{\omega^1, \omega^2, \ldots, \omega^W\}$ be the set of basic transactions in the system.

We study the response of the active line flow $\underline{\boldsymbol{f}}$ to changes in nodal injections $\underline{\boldsymbol{p}}$. Denote the system state by $\underline{\boldsymbol{s}} \triangleq \left[\underline{\boldsymbol{\theta}}^T, \underline{\boldsymbol{V}}^T\right]^T$ with $\underline{\boldsymbol{\theta}} \triangleq [\theta_1, \theta_2, \ldots, \theta_N]^T (\underline{\boldsymbol{V}} \triangleq [V_1, V_2, \ldots, V_N]^T)$ being the voltage phase angle (magnitude) vector. Denote the reference conditions by $\underline{\boldsymbol{p}}^{(0)}$, $\underline{\boldsymbol{q}}^{(0)}$, $\underline{\boldsymbol{s}}^{(0)}$ and $\underline{\boldsymbol{f}}^{(0)}$ that satisfy

$$\begin{cases} \begin{bmatrix} \underline{\boldsymbol{p}}^{(0)} \\ \underline{\boldsymbol{q}}^{(0)} \end{bmatrix} = \begin{bmatrix} \underline{\boldsymbol{g}}_P\left(\underline{\boldsymbol{s}}^{(0)}\right) \\ \underline{\boldsymbol{g}}_Q\left(\underline{\boldsymbol{s}}^{(0)}\right) \end{bmatrix} \triangleq \underline{\boldsymbol{g}}\left(\underline{\boldsymbol{s}}^{(0)}\right) \\ \underline{\boldsymbol{f}}^{(0)} = \underline{\boldsymbol{h}}\left(\underline{\boldsymbol{s}}^{(0)}\right), \end{cases} \tag{1}$$

where $\underline{\boldsymbol{g}}_P(\bullet)/\underline{\boldsymbol{g}}_Q(\bullet)$ represent the active/reactive power flow equations and the component ℓ of $\underline{\boldsymbol{h}}(\bullet)$ is the expression for the active flow in line $\ell \in \mathcal{L}$. We assume the reactive injection remains constant. For a small change $\underline{\Delta\boldsymbol{p}}$ that changes the injection from $\underline{\boldsymbol{p}}^{(0)}$ to $\underline{\boldsymbol{p}}^{(0)} + \underline{\Delta\boldsymbol{p}}$, we denote by $\underline{\Delta\boldsymbol{s}}\,(\underline{\Delta\boldsymbol{f}})$ the corresponding changes in the state $\underline{\boldsymbol{s}}$ (active line flows $\underline{\boldsymbol{f}}$). We assume the system stays in balance and neglect the changes in losses so that, for every *MW* increase in the injection at node $n \neq 0$, there is a corresponding *MW* increase in the withdrawal at the slack node 0 (i.e., $\Delta p_0 = -\sum_{n \in \mathcal{N}, n \neq 0} \Delta p_n$). We apply the first order Taylor's series expansion about $\underline{\boldsymbol{s}}^{(0)}$: See the equation at the bottom of the page.For "small" $\underline{\Delta\boldsymbol{p}}$, $\underline{\Delta\boldsymbol{s}}$ is "small" and so we neglect the higher order terms $(\overline{h.o.t})$. We assume $\underline{\boldsymbol{J}}\left(\underline{\boldsymbol{s}}^{(0)}\right) \triangleq \partial\underline{\boldsymbol{g}}/\partial\underline{\boldsymbol{s}}\big|_{\underline{\boldsymbol{s}}^{(0)}}$ is nonsingular and henceforth drop the bar in the notation so that

$$\underline{\Delta\boldsymbol{s}} \approx \underline{\boldsymbol{J}}^{-1}\left(\underline{\boldsymbol{s}}^{(0)}\right)\begin{bmatrix} \underline{\Delta\boldsymbol{p}} \\ \underline{\boldsymbol{0}} \end{bmatrix} = \underline{\boldsymbol{J}}^{-1}\left(\underline{\boldsymbol{s}}^{(0)}\right)\begin{bmatrix} \underline{\boldsymbol{I}} \\ \underline{\boldsymbol{0}} \end{bmatrix}\underline{\Delta\boldsymbol{p}} \tag{2}$$

$$\underline{\Delta\boldsymbol{f}} \approx \frac{\partial\underline{\boldsymbol{h}}}{\partial\underline{\boldsymbol{s}}}\underline{\Delta\boldsymbol{s}} = \frac{\partial\underline{\boldsymbol{h}}}{\partial\underline{\boldsymbol{s}}}\underline{\boldsymbol{J}}^{-1}\left(\underline{\boldsymbol{s}}^{(0)}\right)\begin{bmatrix} \underline{\boldsymbol{I}} \\ \underline{\boldsymbol{0}} \end{bmatrix}\underline{\Delta\boldsymbol{p}}. \tag{3}$$

The *sensitivity matrix* in (3) depends on $\underline{\boldsymbol{s}}^{(0)}$ and this dependence on the system operating point makes it less than practical for power system applications.

To simplify the computation of the sensitivity matrix, we next introduce the assumptions used in the derivation of dc power flow models and make use of the reduced nodal susceptance matrix [10], $\underline{\boldsymbol{B}} \triangleq \underline{\boldsymbol{A}}^T\underline{\boldsymbol{B}}'\underline{\boldsymbol{A}}$, where $\underline{\boldsymbol{B}}' \triangleq \mathrm{diag}\,[b_1, b_2, \ldots, b_L]$ is the diagonal branch susceptance matrix and $\underline{\boldsymbol{A}} \triangleq [\underline{\boldsymbol{a}}_1, \underline{\boldsymbol{a}}_2, \ldots, \underline{\boldsymbol{a}}_L]^T \in \mathbb{R}^{L \times N}$ is the branch-to-node incidence matrix with $a_\ell^T \triangleq [0 \cdots 0 \;\; \overset{i}{1} \;\; 0 \cdots 0 \;\; \overset{j}{-1} \;\; 0 \cdots 0]$ as row ℓ. We assume $b_\ell \neq 0$, $\ell = 1, 2, \ldots, L$ and $\underline{\boldsymbol{A}}$ to have rank N so that $\underline{\boldsymbol{B}}$ is nonsingular. Under all of these assumptions, $\underline{\boldsymbol{s}}$ reduces to $\underline{\boldsymbol{\theta}}$ and the expressions for the partial derivatives become $\partial\underline{\boldsymbol{g}}_P/\partial\underline{\boldsymbol{\theta}} \approx \underline{\boldsymbol{B}}$, $\partial h_\ell/\partial\underline{\boldsymbol{\theta}} \approx b_\ell\underline{\tilde{\boldsymbol{a}}}_\ell$. It follows that:

$$\underline{\Delta\boldsymbol{f}} \approx \underline{\boldsymbol{B}}'\underline{\boldsymbol{A}}\underline{\boldsymbol{B}}^{-1}\underline{\Delta\boldsymbol{p}} \triangleq \underline{\boldsymbol{\Psi}}\underline{\Delta\boldsymbol{p}}. \tag{4}$$

We henceforth replace the approximation by the equality

$$\underline{\Delta\boldsymbol{f}} = \underline{\boldsymbol{\Psi}}\underline{\Delta\boldsymbol{p}}. \tag{5}$$

The $L \times N$ matrix $\underline{\boldsymbol{\Psi}} \triangleq [\psi_{\ell n}]$ is an approximation of the sensitivity matrix and is called the injection shift factor (*ISF*) matrix. Since $\underline{\boldsymbol{B}}'$, $\underline{\boldsymbol{A}}$ and $\underline{\boldsymbol{B}}$ are solely determined by the network topology/parameters, $\underline{\boldsymbol{\Psi}}$ is independent of $\underline{\boldsymbol{s}}^{(0)}$. The *ISF* of a line $\ell \in L$ with respect to a change in injection at node $n \in \mathcal{N} - \{0\}$ is the element $\psi_{\ell n}$ in row ℓ, column n of $\underline{\boldsymbol{\Psi}}$. Note that $\psi_{\ell n}$ is defined implicitly under the assumption that there is a corresponding change Δp_0 in the injection at the slack node 0 with $\Delta p_0 = -\Delta p_n$. Therefore, the *ISF* is dependent on the slack bus. As the slack bus location changes, the *ISF*s may change. The notion of the *ISF* may be extended to include the slack bus 0. Since the injection and withdrawal buses are identical in this case, $\psi_{\ell 0} \equiv 0$ for all $\ell \in \mathcal{L}$.

$$\begin{cases} \begin{bmatrix} \underline{\boldsymbol{p}}^{(0)} + \underline{\Delta\boldsymbol{p}} \\ \underline{\boldsymbol{q}}^{(0)} \end{bmatrix} = \underline{\boldsymbol{g}}(\underline{\boldsymbol{s}}^{(0)} + \underline{\Delta\boldsymbol{s}}) = \underline{\boldsymbol{g}}(\underline{\boldsymbol{s}}^{(0)}) + \frac{\partial\underline{\boldsymbol{g}}}{\partial\underline{\boldsymbol{s}}}\Big|_{\underline{\boldsymbol{s}}^{(0)}}\underline{\Delta\boldsymbol{s}} + h.o.t. \\ \underline{\boldsymbol{f}}^{(0)} + \underline{\Delta\boldsymbol{f}} = \underline{\boldsymbol{h}}(\underline{\boldsymbol{s}}^{(0)} + \underline{\Delta\boldsymbol{s}}) = \underline{\boldsymbol{h}}(\underline{\boldsymbol{s}}^{(0)}) + \frac{\partial\underline{\boldsymbol{h}}}{\partial\underline{\boldsymbol{s}}}\Big|_{\underline{\boldsymbol{s}}^{(0)}}\underline{\Delta\boldsymbol{s}} + h.o.t. \end{cases}$$

We denote by $\mathcal{H}(n)$ the set of nodes that are connected to node n. A line $\ell = (i,j)$ is radial if either $\mathcal{H}(i) = \{j\}$ or $\mathcal{H}(j) = \{i\}$. For the radial line ℓ with $\mathcal{H}(i) = \{j\}, i \neq 0$

$$\psi_{\ell n} = \begin{cases} 1 & \text{if } n = i \\ 0 & \text{otherwise} \end{cases} \tag{6}$$

since the only impact on line ℓ is due to the injection at node i. For any other line $\ell' \neq \ell$, the injection change at the terminal nodes i and j has the same impact

$$\psi_{\ell' i} = \psi_{\ell' j} \quad \forall\, \ell' \neq \ell. \tag{7}$$

In many applications, we are interested in the impacts of a change Δt in the quantity t of a basic transaction $\omega = \{m, n, t\}$ on the active line flows in an arbitrary line ℓ. This is obtained by setting $\Delta p_m = \Delta t = -\Delta p_n$ and computing the corresponding active flow changes in line ℓ from

$$\Delta f_\ell = \psi_{\ell m}\Delta p_m + \psi_{\ell n}\Delta p_n = (\psi_{\ell m} - \psi_{\ell n})\Delta t. \tag{8}$$

The *ISF* difference term is called the power transfer distribution factor (*PTDF*) of line ℓ with respect to the basic transaction ω and is defined by

$$\varphi_\ell^\omega \triangleq \frac{\Delta f_\ell}{\Delta t} = \psi_{\ell m} - \psi_{\ell n}. \tag{9}$$

In this case, the compensation at the slack bus cancels out since $\Delta p_0 = -(\Delta p_m - \Delta p_n) = 0$. As such, the *PTDF* is independent of the slack bus.

Clearly, both the *ISF*s and *PTDF*s are defined to be small-signal sensitivities. In many applications, however, they are also used to compute large-signal quantities. For example, the total power flow in a line is often evaluated using the *ISF*s by simply replacing the $\underline{\Delta \boldsymbol{f}}(\underline{\Delta \boldsymbol{p}})$ by $\underline{\boldsymbol{f}}(\underline{\boldsymbol{p}})$ in (5).

The *ISF*s and the *PTDF*s have wide applications in congestion modeling. We next explore their role in *CRR* applications.

III. Role in Congestion Revenue Rights Applications

CRR are used once the day-ahead hourly market outcomes are determined. Our discussion focuses on the day-ahead market for a specified hour h. The model of the *LMP*-based day-ahead market is given in Appendix A. In this market, a basic transaction $\omega = \{m, n, t\}$ is required to pay the congestion charges for the corresponding transmission services in the amount of

$$\varsigma = (\mu_n^* - \mu_m^*)t \tag{10}$$

where $\mu_n^*(\mu_m^*)$ represents the *LMP* at node $n(m)$ determined in the day-ahead market [4], [6]. Since the *LMP*s are unknown at the time when the transaction is arranged, this scheme exposes each bilateral transaction to uncertain congestion charges. Transmission customers may hold *CRR* for protection against such uncertainty.

CRR are financial instruments issued by the *IGO* that entitle the holder to be reimbursed for the congestion charges collected by the *IGO*. The implementation of *CRR* requires appropriate modeling of the transmission network. The distribution factors play a key role in the approximations needed in the modeling. We focus on two representative *CRR*—the fixed transmission rights (*FTR*) [6], [7] for the point-to-point rights and the flowgate rights (*FGR*) [8] representing the flow-based rights—and investigate the role and effectiveness of the distribution factors in *CRR* applications.

The *FTR* may be characterized by the *from* node m, the *to* node n, the specified *MW* amount γ and the per *MW* premium ρ. We denote the *FTR* by the quadruplet

$$\boldsymbol{\Gamma} \triangleq \{m, n, \gamma, \rho\}. \tag{11}$$

FTR are issued by the *IGO* and the holder is entitled to receive reimbursement in the amount $(\mu_n^* - \mu_m^*)\gamma$ from the *IGO*.

The network model is incorporated in the *FTR* applications via the so-called simultaneous feasibility test (*SFT*). We denote by $\{\Gamma_k : k = 1, 2, \ldots, K\}$ the set of all the outstanding *FTR*. The *SFT* considers each $\Gamma_k = \{m_k, n_k, \gamma_k, \rho_k\}$ in this set as a fictitious basic transaction $\tilde{\omega}_k \triangleq \{m_k, n_k, \gamma_k\}$ and ensures that the transmission system can accommodate all such transactions simultaneously under the base case and all of the considered contingency conditions. For simplicity, we consider the active power line flow limits $f_\ell^{\max}$ under only the base case so that the *SFT* constraints are expressed as

$$\sum_{k=1}^{K} \gamma_k \varphi_\ell^{\tilde{\omega}_k} \leq f_\ell^{\max} \quad \forall\, \ell \in \mathcal{L}, \tag{12}$$

where the *PTDF*s $\varphi_\ell^{\tilde{\omega}_k}$ are used to evaluate the active line flow in line ℓ induced by the transactions $\{\tilde{\omega}_k : k = 1, 2, \ldots, K\}$. The *SFT* constraints cannot be violated in any phase of the issuance and deployment of *FTR*. Consequently, the *PTDF*s play a role in each of these aspects.

We first examine this role in the determination of the *FTR* issuance quantities. *FTR* are issued in a centralized auction run by the *IGO*. In the auction, customers submit bids that indicate the *from* node, *to* node, and desired quantity of the requested *FTR* and the maximum premium they are willing to pay. The *IGO* collects these bids and runs an optimization problem to determine the actual issuance quantity and corresponding premium for each *FTR* request. The optimization model maximizes the *IGO*'s *FTR* premium income subject to the *SFT* constraints. As such, the *FTR* issuance quantities are implicitly impacted by the *PTDF*s.

The *FTR* needs of transmission customers may change over time. The holder of the existing *FTR* $\Gamma = \{m, n, \gamma, \rho\}$ may need an *FTR* with different *from* node m' and *to* node n'. To fulfill such needs, we allow the customer to return Γ to the *IGO* in exchange for the new *FTR* $\Gamma' \triangleq \{m', n', \gamma', \rho'\}$ for no additional costs. For any of the schemes proposed by *FERC* to determine the new quantity γ' [4], a necessary condition is that the reconfigured *FTR* must satisfy the *SFT* constraints

$$\sum_{k=1}^{K} \gamma_k \varphi_\ell^{\tilde{\omega}_k} - \gamma \varphi_\ell^{\tilde{\omega}} + \gamma' \varphi_\ell^{\tilde{\omega}'} \leq f_\ell^{\max}, \quad \forall\, \ell \in L \tag{13}$$

or, equivalently

$$\gamma' \leq \min_{\ell \in \mathcal{L}, \varphi_\ell^{\tilde{\omega}'} > 0} \left\{ \frac{\left(f_\ell^{\max} - \sum\limits_{k=1}^{K} \gamma_k \varphi_\ell^{\tilde{\omega}_k} + \gamma \varphi_\ell^{\tilde{\omega}} \right)}{\varphi_\ell^{\tilde{\omega}'}} \right\} \tag{14}$$

where $\tilde{\omega}' \triangleq \{m', n', \gamma'\}$. Therefore, the maximum quantity of the reconfigured *FTR* is an explicit function of the *PTDF*s.

SFT constraints are also critical to guarantee the *IGO* revenue adequacy. As shown in Appendix A, the revenues that the *IGO* uses to pay to the *FTR* holders come from two sources: the congestion charges collected from all of the bilateral transactions and the *merchandising surplus* [14] from the market. Let $p_n^{b*}(p_n^{s*})$ be the energy bought from (sold to) the *IGO* at node n in the day-ahead market. The total *IGO* revenues are

$$\xi^{total} = \sum_{n=0}^{N} \mu_n \left(p_n^{b*} - p_n^{s*}\right) + \sum_{w=1}^{W} (\mu_{n^w}^* - \mu_{m^w}^*)t^w. \quad (15)$$

On the other hand, the *IGO* reimburses the *FTR* holders

$$\zeta^{total} = \sum_{k=1}^{K} (\mu_{n_k}^* - \mu_{m_k}^*)\gamma_k. \quad (16)$$

Using the model in the Appendix, it is straightforward to prove that, if the *FTR* satisfy the *SFT*, the *IGO*'s revenues satisfy

$$\xi^{total} \geq \zeta^{total}. \quad (17)$$

Note that this relationship is derived using the *PTDF* approximations. Therefore, the robustness of the *PTDF*s impacts the validity of this inequality.

We next investigate the role of the *PTDF*s in the *FGR*. We consider an arbitrary transaction $\omega = \{m, n, t\}$. As shown in Appendix A, the congestion charges assessed from ω is the *PTDF* weighted sum of the congestion collections on all the congested lines

$$\varsigma = (\mu_n^* - \mu_m^*)t = \sum_{\ell \in \tilde{\mathcal{L}}} \lambda_\ell^* \varphi_\ell^\omega t, \quad (18)$$

where $\tilde{\mathcal{L}}$ is the set of congested lines and λ_ℓ^* is the per *MW* congestion collection for the usage of line ℓ. *FGR* are financial tools that reimburse the holder the congestion collection associated with the specified line in the specified direction [1]. *FGR* may be issued by not only the *IGO* but also the customers who undertake a transaction that provides counterflow in a congested line [8]. We characterize the *FGR* by the specified line ℓ, the indicated node m of the line as the *from* node, the specified *MW* amount σ and the per *MW* premium ρ. We denote the *FGR* by the quadruplet

$$\Sigma \triangleq \{\ell, m, \sigma, \rho\}. \quad (19)$$

Note that the direction of the *FGR* may be different from the physical flow [8]. Hence, for line $\ell = (i, j)$, either $m = i$ or $m = j$. If line ℓ is congested in the specified direction, the holder of Σ receives $\lambda_\ell^* \sigma$ from the issuer. Such payments do not apply if congestion occurs in the opposite direction.

To fully hedge the congestion charges for ω, a customer needs *FGR* for any one of the lines that may become congested. We assume the set of congested lines $\tilde{\mathcal{L}}$ is correctly forecasted. Then, the so-called *FGR* portfolio—the *FGR* set $\left\{\Sigma_u = \{\ell_u, m_u, \sigma_u, \rho_u\} : \ell_u \in \tilde{\mathcal{L}}\right\}$—is constructed with

$$\sigma_u = \varphi_{\ell_u}^\omega t, \quad \forall\, \ell_u \in \tilde{\mathcal{L}}. \quad (20)$$

It follows from (18) that the total payment associated with the *FGR* portfolio reimburses the congestion charges for ω. Note that σ_u may be negative for $\varphi_{\ell_u}^\omega < 0$, which indicates that the flow associated with ω is in the opposite direction of the net flow in the line ℓ_u. Such flow helps to relieve the congestion in the line. Therefore, the customer may sell *FGR* in the amount $|\sigma_u|$ [8].

*PTDF*s are important in the determination of the issuance quantities, the guarantee of the *IGO* revenue adequacy, the implementation of the reconfiguration scheme for the *FTR*, and the construction of *FGR* portfolio. Since the *FTR*/*FGR* issuance occurs before the day-ahead energy market clears, the *PTDF*s used in (12), (14), and (20) may be different from those used in the day-ahead market model given in Appendix A. The statements of this section are based on the assumption that these two sets of *PTDF*s are identical. In practice, however, *PTDF* errors are inevitable. We next study the nature of these errors and their impacts in *FTR*/FGR applications.

IV. PTDF Error Impacts

The distribution factors are evaluated for a given topology and parameter values. In practice, however, the topology/parameters of the forecasted network may change after the *FTR*/*FGR* issuance. Consequently, the *PTDF*s used in the day-ahead market may be different from those in the *FTR*/*FGR* issuances. We refer to this difference as the *PTDF* errors.

We first consider the impacts of changes in network parameters on the values of the *PTDF*s. Let us denote by $\hat{\mathcal{L}} \triangleq \{\hat{\ell}_1, \hat{\ell}_2, \ldots, \hat{\ell}_{\hat{L}}\} \subseteq \mathcal{L}$ the subset of lines whose parameters change after *FTR*/*FGR* issuance. For each line $\hat{\ell} \in \hat{\mathcal{L}}$, the line susceptance changes from $b_{\hat{\ell}}$ to $b_{\hat{\ell}} + \Delta b_{\hat{\ell}}$ with $\Delta b_{\hat{\ell}} \neq 0$. We construct the submatrices of $\underline{\boldsymbol{B}}'$, $\underline{\boldsymbol{A}}$ and $\underline{\boldsymbol{\Psi}}$ corresponding to the lines in $\hat{\mathcal{L}}$ such that $\underline{\boldsymbol{B}}'_{\hat{\mathcal{L}}} \triangleq \text{diag}[b_{\hat{\ell}_1}, b_{\hat{\ell}_2}, \ldots, b_{\hat{\ell}_{\hat{L}}}]$, $\underline{\boldsymbol{A}}_{\hat{\mathcal{L}}} \triangleq [\underline{\boldsymbol{a}}_{\hat{\ell}_1}, \underline{\boldsymbol{a}}_{\hat{\ell}_2}, \ldots, \underline{\boldsymbol{a}}_{\hat{\ell}_{\hat{L}}}]^T$ and $\underline{\boldsymbol{\Psi}}_{\hat{\mathcal{L}}} \triangleq [\underline{\boldsymbol{\psi}}_{\hat{\ell}_1}, \underline{\boldsymbol{\psi}}_{\hat{\ell}_2}, \ldots, \underline{\boldsymbol{\psi}}_{\hat{\ell}_{\hat{\mathcal{L}}}}]^T$. Let $\underline{\boldsymbol{\Delta B}}'_{\hat{L}} \triangleq \text{diag}[\Delta b_{\hat{\ell}_1}, \Delta b_{\hat{\ell}_2}, \ldots, \Delta b_{\hat{\ell}_{\hat{L}}}]$. The changes in $\hat{\mathcal{L}}$ result in changing the $\underline{\boldsymbol{B}}$ matrix into $\underline{\boldsymbol{B}} + \underline{\boldsymbol{A}}_{\hat{\mathcal{L}}}^T \underline{\boldsymbol{\Delta B}}'_{\hat{\mathcal{L}}} \underline{\boldsymbol{A}}_{\hat{\mathcal{L}}}$. This, in turn, changes each row ℓ of $\underline{\boldsymbol{\Psi}}$ by: See the equation (21) at the bottom of the page, which is obtained by applying the Sherman–Morrison–Woodbury formula [15]. We assume $\underline{\boldsymbol{B}}$ and

[1]More generally, *FGR* are associated with flowgates. A flowgate is an interface or corridor which may contain several lines or other transmission facilities. For simplicity, we assume each flowgate contains one line only and, therefore, refers to the flowgate by that line in this paper.

$$\underline{\Delta \boldsymbol{\psi}}_\ell^T = \begin{cases} \frac{\Delta b_\ell}{b_\ell} \underline{\boldsymbol{\psi}}_\ell^T - \frac{b_\ell + \Delta b_\ell}{b_\ell} \underline{\boldsymbol{\psi}}_\ell^T \underline{\boldsymbol{A}}_{\hat{\mathcal{L}}}^T \left(\underline{\boldsymbol{B}}'_{\hat{\mathcal{L}}} \underline{\boldsymbol{\Delta B}}'^{-1}_{\hat{\mathcal{L}}} + \underline{\boldsymbol{\Psi}}_{\hat{\mathcal{L}}} \underline{\boldsymbol{A}}_{\hat{\mathcal{L}}}^T \right)^{-1} \underline{\boldsymbol{\Psi}}_{\hat{\mathcal{L}}}, & \ell \in \hat{\mathcal{L}} \\ -\underline{\boldsymbol{\psi}}_\ell^T \underline{\boldsymbol{A}}_{\hat{\mathcal{L}}}^T \left(\underline{\boldsymbol{B}}'_{\hat{\mathcal{L}}} \underline{\boldsymbol{\Delta B}}'^{-1}_{\hat{\mathcal{L}}} + \underline{\boldsymbol{\Psi}}_{\hat{\mathcal{L}}} \underline{\boldsymbol{A}}_{\hat{\mathcal{L}}}^T \right)^{-1} \underline{\boldsymbol{\Psi}}_{\hat{\mathcal{L}}}, & \ell \notin \hat{\mathcal{L}} \end{cases} \quad (21)$$

$\underline{\boldsymbol{B}}+\underline{\boldsymbol{A}}_{\hat{\mathcal{L}}}^T\underline{\Delta\boldsymbol{B}}'_{\hat{\mathcal{L}}}\underline{\boldsymbol{A}}_{\hat{\mathcal{L}}}$ to be nonsingular so that $\underline{\boldsymbol{B}}'_{\hat{\mathcal{L}}}\underline{\Delta\boldsymbol{B}}'^{-1}_{\hat{\mathcal{L}}}+\underline{\boldsymbol{\Psi}}_{\hat{\mathcal{L}}}\underline{\boldsymbol{A}}_{\hat{\mathcal{L}}}^T$ is invertible [15].

We may view network topology changes, such as line outages and line additions, as special cases of parameter changes. For example, the outage of a single line $\hat{\ell}=(\hat{\imath},\hat{\jmath})$ results in $\hat{\mathcal{L}}=\{\hat{\ell}\}$, $\underline{\boldsymbol{A}}_{\hat{\mathcal{L}}}=\underline{a}_{\hat{\ell}}^T$, and $\Delta b_{\hat{\ell}}=-b_{\hat{\ell}}$, so that

$$\underline{\Delta\boldsymbol{\psi}}_{\ell}^T=\begin{cases}-\underline{\boldsymbol{\psi}}_{\hat{\ell}}^T, & \text{if } \ell=\hat{\ell}\\ \frac{\psi_{\ell\hat{\imath}}-\psi_{\ell\hat{\jmath}}}{1-(\psi_{\hat{\ell}\hat{\imath}}-\psi_{\hat{\ell}\hat{\jmath}})}\underline{\boldsymbol{\psi}}_{\hat{\ell}}^T, & \text{otherwise.}\end{cases} \tag{22}$$

The factor $\phi_{\ell,\hat{\ell}}=\psi_{\ell\hat{\imath}}-\psi_{\ell\hat{\jmath}}/1-(\psi_{\hat{\ell}\hat{\imath}}-\psi_{\hat{\ell}\hat{\jmath}})$ is called line outage distribution factor [10], [11]. The flow change Δf_ℓ for line $\ell\neq\hat{\ell}$ satisfies $\Delta f_\ell=\phi_{\ell,\hat{\mathcal{L}}}f_{\hat{\ell}}$, where $f_{\hat{\ell}}$ is the preoutage line $\hat{\ell}$ flow [2].

Another example is the addition of a line $\hat{\ell}=(\hat{\imath},\hat{\jmath})$. Two possible situations of interest are

i) $\hat{\ell}$ is a radial line with $\hat{\imath}\notin\mathcal{N}$ whose addition results in $\mathcal{L}^a=\mathcal{L}\cup\hat{\ell}$ and $\mathcal{N}^a=\mathcal{N}\cup\hat{\imath}$. We may apply (6) and (7) to construct the augmented *ISF* matrix

$$\underline{\boldsymbol{\Psi}}^a=\begin{bmatrix}\underline{\boldsymbol{\Psi}} & \underline{\boldsymbol{\psi}}^{\hat{\imath}}\\ \underline{\boldsymbol{0}}^T & 1\end{bmatrix} \tag{23}$$

where $\underline{\boldsymbol{\psi}}^{\hat{\imath}}=\underline{\boldsymbol{\psi}}^{\hat{\jmath}}$, the column $\hat{\jmath}$ of $\underline{\boldsymbol{\Psi}}$;

ii) $\hat{\ell}=(\hat{\imath},\hat{\jmath})$ is a new line with $\hat{\imath},\hat{\jmath}\in\mathcal{N}$. Its addition results in the changed line set $\mathcal{L}^a=\mathcal{L}\cup\hat{\ell}$. We define a new *ISF* row vector $\underline{\boldsymbol{\psi}}_{\hat{\ell}}^T\triangleq b_{\hat{\ell}}\underline{\boldsymbol{a}}_{\hat{\ell}}^T\underline{\boldsymbol{B}}$ and construct the augmented $(L+1)\times N$ *ISF* matrix

$$\underline{\boldsymbol{\Psi}}^a=\begin{bmatrix}\underline{\boldsymbol{\Psi}}+\underline{\Delta\boldsymbol{\Psi}}\\ \underline{\boldsymbol{\psi}}_{\hat{\ell}}^T+\underline{\Delta\boldsymbol{\psi}}_{\hat{\ell}}^T\end{bmatrix} \tag{24}$$

where $\underline{\Delta\boldsymbol{\psi}}_{\hat{\ell}}^T$ and each row of $\underline{\Delta\boldsymbol{\Psi}}$ is determined by

$$\underline{\Delta\boldsymbol{\psi}}_{\ell}^T=-\frac{\psi_{\ell\hat{\imath}}-\psi_{\ell\hat{\jmath}}}{1+(\psi_{\hat{\ell}\hat{\imath}}-\psi_{\hat{\ell}\hat{\jmath}})}\underline{\boldsymbol{\psi}}_{\hat{\ell}}^T. \tag{25}$$

Equations (21)–(25) express the *ISF* errors due to network changes. The *PTDF* errors may be evaluated from these results using the linear relationship in (9). We denote by $\varphi_\ell^\omega(\bar{\varphi}_\ell^\omega)$ the *PTDF*s used in the *FTR*/*FGR* issuances (day-ahead market) and study the impacts of the *PTDF* errors

$$\Delta\varphi_\ell^\omega\triangleq\varphi_\ell^\omega-\bar{\varphi}_\ell^\omega \tag{26}$$

in *FTR*/*FGR* applications.

We investigate the impacts of these errors on the *FTR* issuance quantities, which are a function of the *SFT* constraints. Substituting the actual *PTDF*s into (12) yields

$$\sum_{k=1}^{K}\bar{\gamma}_k\bar{\varphi}_\ell^{\tilde{\omega}_k}\leq f_\ell^{\max}\quad\forall\,\ell\in\mathcal{L}. \tag{27}$$

However, the *FTR* quantities $\underline{\boldsymbol{\gamma}}\triangleq[\gamma_1,\gamma_2,\ldots,\gamma_K]^T$ determined using the *PTDF*s $\varphi_\ell^{\tilde{\omega}_k}$ may not satisfy (27). In other words, due to the *PTDF* errors, the *FTR* might be either over issued, making the transmission system not able to accommodate simultaneously all of the possible transactions corresponding to the *FTR*, or conservative so that not all of the transmission capability is used. Let $\underline{\bar{\boldsymbol{\gamma}}}\triangleq[\bar{\gamma}_1,\bar{\gamma}_2,\ldots,\bar{\gamma}_K]^T$ be the vector of the *optimal* issuance quantities corresponding to the *PTDF*s $\bar{\varphi}_\ell^{\tilde{\omega}_k}$. For small *PTDF* errors, the magnitude of the relative error on the *FTR* issuance quantities

$$\varepsilon^\gamma\triangleq\frac{\|\underline{\boldsymbol{\gamma}}-\underline{\bar{\boldsymbol{\gamma}}}\|}{\|\underline{\bar{\boldsymbol{\gamma}}}\|} \tag{28}$$

is bounded by a small number. This is proved in Appendix B.

We next focus on the *IGO* revenue adequacy. The inequality in (17) is derived based on the assumption that the *PTDF*s used in the *SFT* and the day-ahead market are identical. Due to the *PTDF* errors, this assumption no longer holds. Consequently, the *IGO*'s revenue adequacy is not guaranteed when there are *PTDF* errors. While analytical evaluations of the revenue shortfall introduced by these errors are difficult, we examine such impacts from simulations in Section V.

The *PTDF* errors may also impact the hedging ability of the *FGR* portfolios. Due to *PTDF* errors, the *FGR* portfolios constructed based on the *PTDF*s φ_ℓ^ω may not be able to fully hedge the transaction. Consider the *FGR* portfolio constructed for the transaction $\omega=\{m,n,1\}$. The *FGR* quantities satisfy

$$\sigma_u=\varphi_{\ell_u}^\omega,\quad\forall\,\ell_u\in\tilde{L}. \tag{29}$$

The total reimbursements of this *FGR* portfolio are

$$\pi=\sum_{\ell_u\in\tilde{\mathcal{L}}}\lambda_{\ell_u}\sigma_u=\sum_{\ell\in\tilde{\mathcal{L}}}\lambda_\ell\varphi_\ell^\omega. \tag{30}$$

The actual congestion charges for ω are

$$\varsigma=\mu^n-\mu^m=\sum_{\ell\in\tilde{\mathcal{L}}}\lambda_\ell\bar{\varphi}_\ell^\omega. \tag{31}$$

Since the relative error

$$\varepsilon^\pi\triangleq\left|\frac{\varsigma-\pi}{\varsigma}\right|=\frac{\left|\sum_{\ell\in\tilde{\mathcal{L}}}\lambda_\ell\left(\bar{\varphi}_\ell^\omega-\varphi_\ell^\omega\right)\right|}{\left|\sum_{\ell\in\tilde{\mathcal{L}}}\lambda_\ell\bar{\varphi}_\ell^\omega\right|}\leq\max_{\ell\in\tilde{\mathcal{L}}}\left\{\left|\frac{\Delta\varphi_\ell^\omega}{\bar{\varphi}_\ell^\omega}\right|\right\} \tag{32}$$

an upper bound is obtained. The value of this bound could be large under certain conditions. However, in most cases, the relative error in (32) is primarily due to the errors associated with large-valued *PTDF*s. As we illustrate in Section V, large *PTDF*s are typically associated with small relative errors. Therefore, the relative differences between the *FGR* reimbursements and the congestion charges are, typically, small.

V. Simulation Results

To investigate the quality and robustness of the distribution factors in *FTR*/*FGR* applications, we have simulated various cases on a number of test systems including the IEEE 118-bus system and portions of the U.S. Eastern Interconnection. In this section, we summarize representative results of our studies.

[2]The term $\psi_{\hat{\ell}\hat{\imath}}-\psi_{\hat{\ell}\hat{\jmath}}=1$ only when $\{\ell\}$ is a cutset of the network [15] that separates the system into two subnetworks. In such a case, the *ISF*s need to be redefined for each subnetwork.

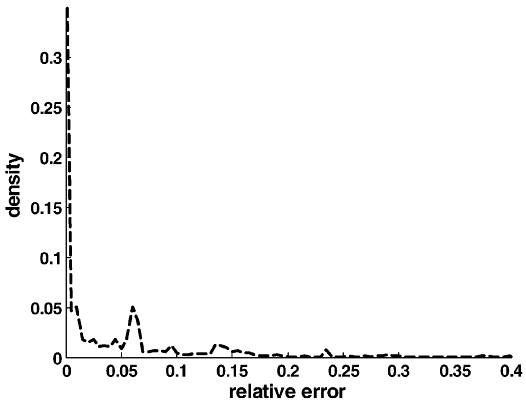

a. the *PTDF* error density function for the set (a) of 50% reactance cases

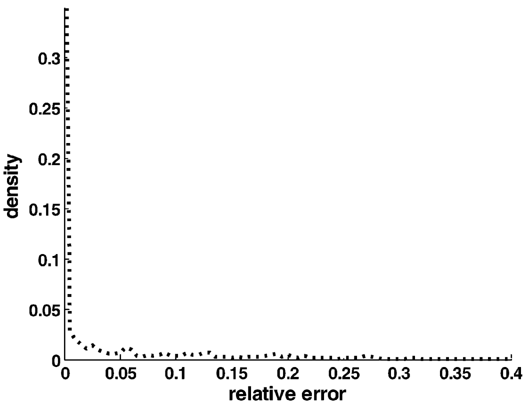

b. the *PTDF* error density function for the set (b) of line outage cases

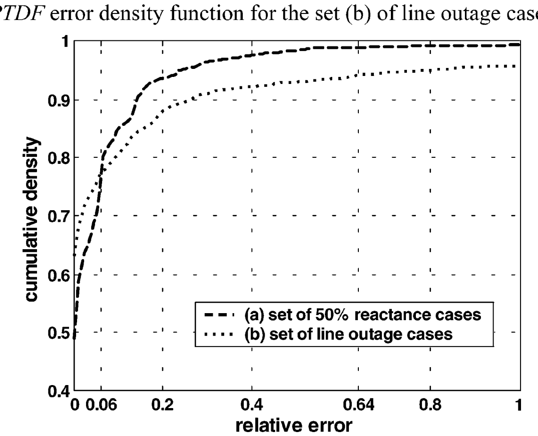

c. the cumulative distribution functions of the relative errors

Fig. 1. *PTDF* error density functions for the two sets of results and the corresponding cumulative distribution functions.

We designate the base case as the conditions used to forecast the *PTDF*s for the *FTR*/*FGR* issuances. The network that determines the *PTDF*s used in the day-ahead market is represented by various changes in the network topology/parameters. We provide representative results by generating two sets of cases based on the IEEE 118-bus system

a) the set of 50% reactance cases: for each line in the set $\{$ (4,11), (8,30), (11,13), (15,33), (23,24), (24,70), (25,26), (25,27), (26,30), (37,34), (46,45), (49,51), (55,59), (65,38), (68,81), (69,77), (76,118), (88,85), (89,92), (113,31) $\}$, we decrease to 50% the line reactance, one line at a time, and construct the set of corresponding cases;

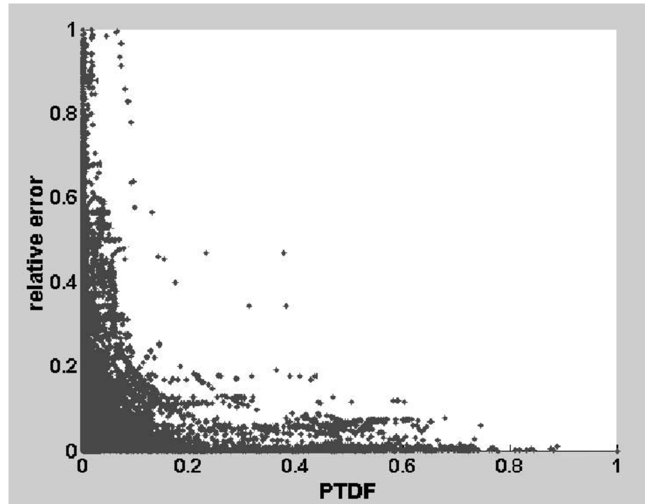

Fig. 2. Scatter plot of the relative errors as a function of the *PTDF* magnitudes.

b) the set of line outage cases: for each line in the set above, we simulate its outage, one line at a time and construct the corresponding set of cases; the resulting set is used to study $n-1$ security.

We first investigate the *PTDF* errors introduced by the changes in the network topology and parameters. For each case in the sets (a) and (b), we compute the *PTDF* for every pair of nodes in the system and compare to the value of the base case. We compute the relative errors for each *PTDF*

$$\varepsilon \triangleq \left| \frac{\left(\varphi_\ell^\omega - \bar{\varphi}_\ell^\omega\right)}{\bar{\varphi}_\ell^\omega} \right|. \tag{33}$$

We collect the errors and construct a density function for each set of results and then construct the corresponding cumulative distribution function, as shown in Fig. 1. The plots in Fig. 1(a) and (b) show that the frequency for the relative errors is high for small errors but rather low for large errors for the two sets of cases studied. These plots make clear that, although the parameter/topology changes in the network may result in major impacts on the value of some particular *PTDF*s, the fraction of *PTDF*s that are impacted is relatively small. The side-by-side comparison of the cumulative distribution functions shown in Fig. 1(c) allows us to assess the impacts of parameter changes versus line outages. Typically, line outages have more impacts on the *PTDF* values than parameter changes. For some specific lines, a parameter change will introduce a small—less than 0.1—*PTDF* error while the outage of that line may result in a significant *PTDF* error. The scatter plot in Fig. 2 shows the size of relative error as a function of the corresponding *PTDF* magnitude. This plot reinforces the notion that large errors are associated primarily with small magnitude *PTDF*s.

Next, we investigate the effectiveness of the *PTDF*s in the evaluation of the total active line flow. We use the ac power flow results for benchmark purposes and evaluate the absolute value of the relative errors

$$\varepsilon^f \triangleq \left| \frac{\left(f_\ell^{PTDF} - f_\ell^{AC}\right)}{f_\ell^{AC}} \right| \tag{34}$$

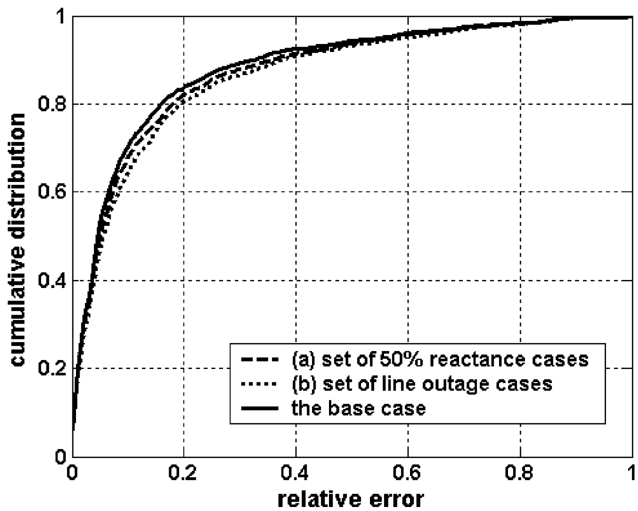

Fig. 3. Cumulative distribution functions of the relative errors in the line flow approximations.

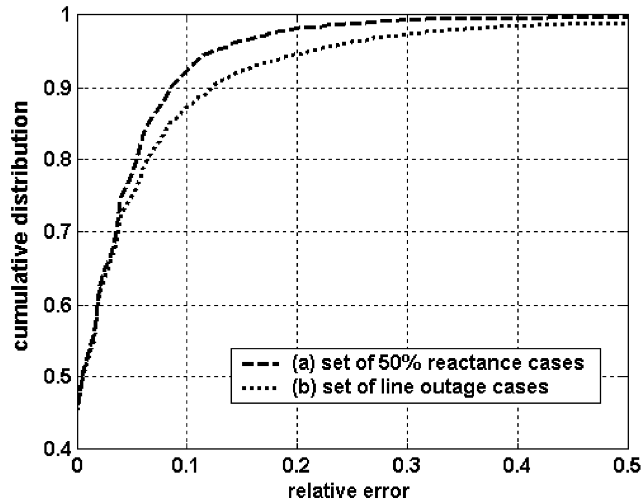

Fig. 4. Cumulative distribution functions of the *FTR* issuance quantity errors.

where f_ℓ^{PTDF} is the active line flow in line ℓ evaluated using the base case *PTDF*s and f_ℓ^{AC} is obtained from the ac power flow results for the base case or the changed network conditions. For the base case and each case in the sets (a) and (b), we vary the load level of the system from 60% to 140% of the base case value and examine the relative errors. We collect these errors and evaluate their distributions. We show representative cumulative distribution functions in Fig. 3. The plots indicate that the relative errors are above 0.2 in about 20% of cases studied. Such errors are observed under both the changed network conditions and the base case condition. We, therefore, conclude that the errors are introduced by the linearization approximation in the derivation of the *PTDF*s. The closeness of the three curves was observed in all of the simulation tests for the large number of different systems tested. These results lead to the experimentally observed conclusion that changes in network topology/parameters do not result in major impacts on the accuracy of *PTDF* approximations of the line flows.

To check the *PTDF* error impacts on the *FTR* issuance quantities, we consider a set of *FTR* requests and determine the issuance quantities based on the base case *PTDF*s and the *PTDF*s for each case in the sets (a) and (b). We compare the results and evaluate the relative errors ε^γ. We repeat this test for various sets of requests and collect all of the errors. We evaluate the distribution of these errors and show representative cumulative distribution functions in Fig. 4. This plot indicates that the impacts on the *FTR* issuance quantities of the *PTDF* errors due to the network topology/parameter changes are small. In both sets (a) and (b), the relative errors are smaller than 10% for more than 90% of the cases.

We also list some representative statistical results in Table I to illustrate that changes in each of the congested lines have relatively major impacts on the *FTR* issuance quantities while the impacts of the changes in the other lines are limited.

We next examine the *IGO* revenue adequacy for the various cases. Our results indicate that the *IGO* has revenue adequacy

TABLE I
RELATIVE ERRORS IN THE FTR ISSUANCE QUANTITIES

set of cases \ variation in	congested lines		uncongested lines		all lines	
	average	maximum	average	maximum	average	maximum
(a)	0.052	5.472	0.028	0.434	0.0387	5.472
(b)	0.098	7.467	0.055	3.515	0.0741	7.467

in most of the cases studied. The *IGO* revenues are less than the *FTR* reimbursements in less than 12% of all the cases studied. Each such inadequate revenue case corresponds to a case where the *SFT* constraints of (27) are violated. Our simulations indicate that, on the average, the *IGO* revenues exceed the *FTR* reimbursements. As such, over a given period, it is reasonable to expect that there is revenue adequacy. In fact, this finding may be the rationale used by *PJM* for performing the *FTR* settlements on a monthly basis [7]. The monthly calculations attenuate the impacts of the *PTDF* errors.

We also study the impacts of the *PTDF* errors on the hedging ability of the *FGR* portfolios. We construct *FGR* portfolios for a set of transactions based on the base case *PTDF*s. For each case in the sets (a) and (b), we compute the actual reimbursements π of this portfolio and compare it with the congestion charges ς associated with the transaction. We compute the magnitudes of the relative differences ε^π. We collect these errors and evaluate their distributions. The resulting cumulative distribution functions are illustrated in Fig. 5. The results shown in Fig. 5 are representative of our findings that the *FGR* portfolios constructed using the base case *PTDF*s can provide satisfactory hedging ability in most of the cases even for the presence of *PTDF* errors due to changes in the network topology/parameters. There are, however, around 5% of the cases in which the relative errors are significant. Such situations typically occur when a congested line ℓ with large λ_ℓ^* is outaged or undergoes a parameter change.

To conclude, our simulations indicate that the impacts of the *PTDF* errors in the *FTR*/*FGR* applications stay in an acceptable range under a broad spectrum of conditions.

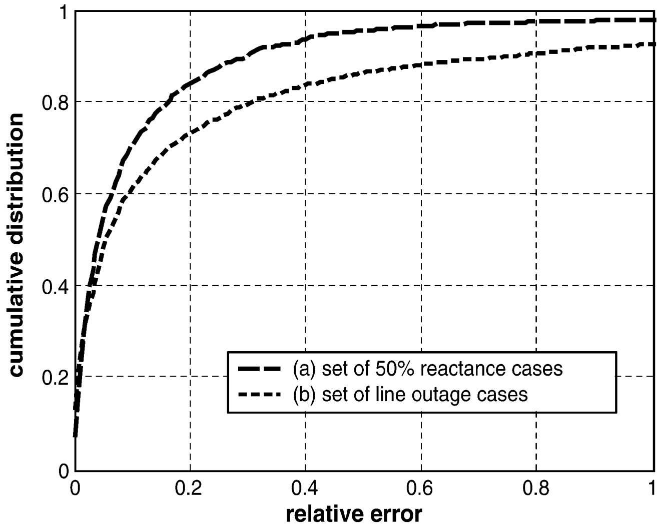

Fig. 5. Cumulative distribution functions of the *FGR* portfolio hedging errors.

VI. Summary

In this paper, we investigated the role and effectiveness of the distribution factors—the *ISF*s and *PTDF*s—in *CRR* applications. We analyzed the characteristics of these distribution factors and examined the range of conditions over which these factors can provide reliable approximations for large power system networks.

PTDF errors impact all aspects of *CRR* applications: *FTR* issuance quantities, *IGO* revenue adequacy, and hedging ability of the *FGR* portfolios. We investigated these impacts and derived analytical bounds on the relative errors. Numerical results indicate that the impacts are minor under a broad spectrum of conditions including contingencies used to establish $n-1$ *security*. This paper does not consider the impacts of the losses in the modeling of transmission. The incorporation of the transmission losses is a natural extension of the work reported here.

Appendix A
Day-Ahead Market Model

We consider the integrated day-ahead market operated by the *IGO* for hour h. Since all of the discussion pertains to hour h, we suppress the time notation in this paper. In this market, the *pool customers*—the entities who buy (sell) energy directly from (to) the *IGO*—submit their energy sale offers/purchase bids to the *IGO*. Without loss of generality, we assume one seller and one buyer at each node $n \in \mathcal{N}$ and denote by $\beta_n^s(p_n^s)/\beta_n^b(p_n^b)$ the seller's offer/buyer's bid price as a function of the active power supply/consumption. We define $\underline{\boldsymbol{p}}^s \triangleq [p_1^s, p_2^s, \ldots, p_N^s]^T$ and $\underline{\boldsymbol{p}}^b \triangleq [p_1^b, p_2^b, \ldots, p_N^b]^T$. The *IGO* determines successful offers/bids by maximizing the total social welfare [5] subject to the network constraints.

The transmission services of the bilateral transactions $\{\omega^1, \omega^2, \ldots, \omega^W\}$ are also scheduled in this market. For each bilateral transaction $\omega^w = \{m^w, n^w, t^w\}$, there is an entity that requests the required transmission services from the *IGO*. We call such an entity a *bilateral transmission customer*. The extent to which each transmission service request is met depends on the customer's willingness to pay the congestion charges. We assume all bilateral customers are willing to pay the charges—no matter how high—so that all of their transactions are scheduled. The bilateral transactions introduce active power injections p_n^t at each node n with

$$p_n^t = \sum_{w=1}^{W} t^w \Bigg|_{m^w=n} - \sum_{w=1}^{W} t^w \Bigg|_{n^w=n}, \quad n = 0, 1, 2, \ldots, N. \tag{A.1}$$

Let $\underline{\boldsymbol{p}}^t \triangleq [p_1^t, p_2^t, \ldots, p_N^t]^T$. Then, the *IGO*'s process to determine the successful bids/offers may be formulated as the so-called transmission scheduling problem (TSP)

$$TSP \begin{cases} \max & s(p_0^s, p_0^b, \underline{\boldsymbol{p}}^s, \underline{\boldsymbol{p}}^b) \triangleq \sum\limits_{n=0}^{N} \beta_n^b(p_n^b) - \beta_n^s(p_n^s) \\ \text{s.t.} & p_0^s - p_0^b + p_0^t = \underline{\boldsymbol{b}}_0^T \underline{\boldsymbol{\theta}} \leftrightarrow \mu_0 \\ & \underline{\boldsymbol{p}}^s - \underline{\boldsymbol{p}}^b + \underline{\boldsymbol{p}}^t = \underline{\boldsymbol{B}}\underline{\boldsymbol{\theta}} \leftrightarrow \underline{\boldsymbol{\mu}} \\ & \underline{\boldsymbol{B}}_b \underline{\boldsymbol{A}}\underline{\boldsymbol{\theta}} \leq \underline{\boldsymbol{f}}^{\max} \leftrightarrow \underline{\boldsymbol{\lambda}} \end{cases} \tag{A.2}$$

where s is the total social welfare [5].

The day-ahead market is settled based on the optimal solutions of the TSP, which we assume exist. The optimal values of the decision variables (p_n^{b*}, p_n^{s*}) determine the quantities of the energy purchased from/sold to the pool customers. Prices are determined from the optimal values of the dual variables. μ_n^* is the *LMP* at the node n of the network. A seller (buyer) at each node n is paid (pays) the *LMP* μ_n^* by (to) the *IGO* for each *MW* sold (bought) in the pool. The net income of the *IGO* from the pool $\sum_{n=0}^{N} \mu_n^* \left(p_n^{b*} - p_n^{s*}\right)$, is called the *merchandising surplus* [14]. λ_ℓ^* measures the marginal change in the social welfare with respect to a change in the limiting capacity $f_\ell^{\max}$ of line ℓ. Note that $\lambda_\ell^* \geq 0$ for $\forall\, \ell \in \mathcal{L}$ and $\lambda_\ell^* > 0$ implies that line ℓ is congested. The per *MW* congestion collection of line ℓ is set to be λ_ℓ^*. We denote by $\tilde{\mathcal{L}} \subset \mathcal{L}$, the set of congested lines. The total congestion charges ς assessed from each $\omega = \{m, n, t\}$ is then

$$\varsigma = \sum_{\ell \in \tilde{\mathcal{L}}} \lambda_\ell^* \varphi_\ell^\omega t. \tag{A.3}$$

The optimality conditions for (A.2) lead to the relationship

$$\mu_n^* - \mu_m^* = \sum_{\ell \in \tilde{\mathcal{L}}} \lambda_\ell^* \varphi_\ell^\omega. \tag{A.4}$$

It follows that:

$$\varsigma = (\mu_n^* - \mu_m^*) t, \tag{A.5}$$

that is, ς is the product of transaction amount t and the *LMP* differences between its delivery and receipt node.

We refer the reader to a more detailed discussion of the model in [17].

Appendix B
Error Bound for the FTR Issuance Quantity

In this appendix, we derive an analytical bound for the relative errors in the *FTR* quantities due to the *PTDF* errors. We consider the optimization problem used by the *IGO* to determine the *FTR* issuance quantity that maximizes the *IGO*'s premium income subject to the *SFT* constraints. Due to continuity, there exist $\delta_{\ell k} > 0$ such that if

$$\left|\varphi_\ell^{\tilde{\omega}_k} - \bar{\varphi}_\ell^{\tilde{\omega}_k}\right| \le \delta_{\ell k} \quad \forall\, \ell \in \mathcal{L}, \quad k = 1, 2, \ldots, K, \qquad \text{(B.1)}$$

then the set of lines $\mathcal{L}'$ whose constraints are binding in the *SFT* with the *PTDF*s $\varphi_\ell^{\tilde{\omega}_k}$ of (12) is identical to that with the *PTDF*s $\bar{\varphi}_\ell^{\tilde{\omega}_k}$ given by (27). We assume the *PTDF* errors are sufficiently small so that (B.1) is satisfied. We express these binding constraints by

$$\underline{\boldsymbol{D}}\underline{\boldsymbol{\gamma}} = \underline{\boldsymbol{f}}_B^{\max} = \underline{\bar{\boldsymbol{D}}}\underline{\bar{\boldsymbol{\gamma}}} \qquad \text{(B.2)}$$

where $\underline{\boldsymbol{f}}_B^{\max} \in \mathbb{R}^{|\mathcal{L}'|}$ is the vector of binding flow limits and $\underline{\boldsymbol{D}}(\underline{\bar{\boldsymbol{D}}})$ is the coefficient matrix of the *PTDF*s $\varphi_\ell^{\tilde{\omega}_k}(\bar{\varphi}_\ell^{\tilde{\omega}_k})$. In cases of interest, $\underline{\bar{\boldsymbol{D}}}$ is not ill-conditioned. We view these relations as the solution of equations with a disturbed coefficient matrix. From the theorem given in [16], it follows that:

$$\varepsilon^\gamma = \frac{\|\underline{\boldsymbol{\gamma}} - \underline{\bar{\boldsymbol{\gamma}}}\|}{\|\underline{\bar{\boldsymbol{\gamma}}}\|} \le cond(\underline{\bar{\boldsymbol{D}}})\frac{\|\underline{\boldsymbol{D}} - \underline{\bar{\boldsymbol{D}}}\|}{\|\underline{\bar{\boldsymbol{D}}}\|} \qquad \text{(B.3)}$$

where $cond(\underline{\bar{\boldsymbol{D}}})$ refers to the condition number of $\underline{\bar{\boldsymbol{D}}}$ [16]. For small *PTDF* errors that satisfy (B.1), $\|\underline{\boldsymbol{D}} - \underline{\bar{\boldsymbol{D}}}\| \ll \|\underline{\bar{\boldsymbol{D}}}\|$. Consequently, ε^γ is bounded by a small number.

REFERENCES

[1] E. Bompard, P. Correia, G. Gross, and M. Amelin, "Congestion-management schemes: A comparative analysis under a unified framework," *IEEE Trans. Power Syst.*, vol. 18, pp. 346–352, Feb. 2003.

[2] H. Singh, H. Shangyou, and A. Papalexopoulos, "Transmission congestion management in competitive electricity markets," *IEEE Trans. Power Syst.*, vol. 13, pp. 672–680, May 1998.

[3] P. Gribik, G. A. Angelidis, and R. R. Kovacs, "Transmission access and pricing with multiple separate energy forward markets," *IEEE Trans. Power Syst.*, vol. 14, pp. 865–876, Aug. 1999.

[4] Remedying Undue Discrimination Through Open Access Transmission Service and Standard Electricity Market Design. Federal Energy Regulatory Commission. [Online]. Available: http://www.ferc.gov/Electric/RTO/Mrkt-Strct-comments/nopr/Web-NOPR.pdf.

[5] S. Stoft, *Power System Economics: Designing Markets for Electricity*. Piscataway, NJ: IEEE Press, 2002.

[6] W. Hogan, "Contract networks for electric power transmission," *J. Reg. Econ.*, vol. 4, pp. 211–242, 1992.

[7] PJM Manual for Fixed Transmission Rights. PJM interconnection. [Online]. Available: http://pubs.pjm.com/dynaweb/PJMpubp/m06.

[8] H. Chao, S. Peck, S. Oren, and R. Wilson, "Flow-based transmission rights and congestion management," *Elect. J.*, pp. 38–58, Oct. 2000.

[9] W. Y. Ng, "Generalized generation distribution factors for power system security evaluation," *IEEE Trans. Power App. Syst.*, vol. PAS-100, pp. 1001–1005, Mar. 1981.

[10] A. Wood and B. Wollenberg, *Power Generation Operation and Control*, 2nd ed. New York: Wiley, 1996, pp. 105–108.

[11] *Available Transfer Capability Definitions and Determination*. Princeton, NJ: North American Electric Reliability Council, 1996.

[12] M. Liu and G. Gross, "Effectiveness of the distribution factor approximations used in congestion modeling," in *Proc. 14th Power Syst. Comput. Conf.*, Seville, Spain, June 2002, pp. 24–28.

[13] R. Baldick, "Variation of distribution factors with loading," *IEEE Trans. Power Syst.*, vol. 18, pp. 1316–1323, Nov. 2003.

[14] P. L. Joskow and J. Tirole, "Transmission rights and market power on electric power networks," *RAND J. Econ.*, vol. 31, no. 3, pp. 450–487, Autumn 2000.

[15] L. Chua and P. Lin, *Computer-Aided Analysis of Electronic Circuits: Algorithms & Computational Techniques*. Englewood Cliffs, NJ: Prentice-Hall, 1975, pp. 134–140.

[16] G. Golub and C. Van Loan, *Matrix Computations*. Baltimore, MD: The John Hopkins Univ. Press, 1996, pp. 80–84.

[17] M. Liu and G. Gross, "Framework for the design and analysis of congestion revenue rights," *IEEE Trans. Power Syst.*, vol. 19, pp. 243–251, Feb. 2004.

Minghai Liu (S'03) received the B.S. and M.S. degrees in electrical engineering from Tsinghua University, Beijing, China, in 1997 and 2000, respectively.

Currently, he is a Research Assistant at the University of Illinois at Urbana-Champaign. His research interests include power system operations, control, optimization, and economics.

George Gross (F'88) received the B.S. degree from McGill University, Montreal, QC, Canada, and graduate degrees from the University of California, Berkeley.

Currently, he is Professor of Electrical and Computer Engineering and Professor of the Institute of Government and Public Affairs at the University of Illinois at Urbana-Champaign. He was previously employed by Pacific Gas and Electric Company, San Francisco, CA, in various technical, policy, and management positions. His research and teaching activities are in the areas of power system analysis, planning, economics, and operations and utility regulatory policy and industry restructuring.